Polymer Bulletin (2022) 79:8503–8516
https://doi.org/10.1007/s00289-021-03927-z

ORIGINAL PAPER

Synthesis and characterization of a molecularly ımprinted polymer adsorbent for selective solid-phase extraction from wastewater of propineb

Çiğdem Öter[1] · **Özlem Selçuk Zorer**[1]

Received: 20 July 2021 / Revised: 20 September 2021 / Accepted: 29 September 2021 /
Published online: 7 October 2021

Abstract

Pesticide residues, which have become a critical problem today, negatively affect the living life and cause concern for the future life. Different methods are being developed to eliminate the problems caused by pesticides and pesticide residue analysis. In this study, a new molecularly imprinted polymer (MIP) has been synthesized for using methacrylic acid as the functional monomer and propineb, a fungicide, as the template molecule. The selectivity and binding properties of MIP were compared with non-imprinted polymer (NIP). MIP particles were used as an adsorbent in the solid-phase extraction column, and various extraction parameters were extensively optimized to evaluate the extraction performance. It was determined that under optimum extraction conditions, MIP showed higher selectivity and extraction capacity toward propineb compared to commercial C_{18} column and NIP. As a result, the developed solid phase extraction method was optimized for propineb residue analysis, and high extraction efficiency was obtained. This method, which is low cost, requires very little use of organic solvents, is fast and easy, is selective and environmentally friendly, is very useful for the purification of wastewater from pollutants.

Keywords Fungicides · Kinetic · Solid-phase extraction · Molecularly imprinted polymers · Propineb

Introduction

The excessive use of synthetic chemicals (pesticides) for plant health shows that risk factors for the human, animal and environmental health have increased. Pesticides can pose severe threats to living organisms as they are non-biodegradable, toxic, and carcinogenic [1]. Fungicides are chemical compounds used in agriculture against fungal

✉ Çiğdem Öter
cigdemoter@yyu.edu.tr

[1] Department of Chemistry, Faculty of Science, Van Yuzuncu Yil University, 65080 Van, Turkey

pests. They are used more than herbicides and insecticides. Dithiocarbamates are commonly used to control over 400 pathogens in more than 70 crops due to their wide spectrum of antifungal activity [2, 3]. The effect of direct exposure to these fungicides can cause eye and skin allergies, inflammation of the airways, and asthmatic events in humans. Propineb is a fungicide commonly used in the Mediterranean region due to its low production cost and high activity against fungal plant illness. It has a special goitrogenic effect in rats. In addition, long-term inhalation or oral exposure may cause reproductive dysfunction, carcinogenicity, vital organ dysfunction, and teratogenicity [4, 5]. Thus, it is essential to find efficient and straightforward methods for determining fungicide residuals in environmental samples and foodstuffs [6].

Many methods have been developed in recent years to determine traces of pesticides. Gas chromatography (GC) [7] and GC–MS [8], liquid chromatography (LC) [9], LC-mass spectrometry (LC–MS) [10], solid-phase extraction (SPE) [11] including extraction and pre-concentration steps, solid-phase microextraction (SPME) [12] methods are the most widely used are techniques. In addition, liquid–liquid microextraction (LLME) [13] and phase microextraction (LPME) [14], which are non-selective pretreatment methods for complex matrices, are also used.

SPE is a prevalent type of cleaning technique for bioanalytical purposes due to its simplicity and versatility. The SPE technique is more straightforward, economical, and faster than traditional liquid–liquid extraction [15, 16]. High selectivity sorbents need to be developed to enable the SPE method and add more selective analyte pre-concentrations. Molecularly imprinted polymers (MIPs) appear to be excellent sorbents meeting the high selectivity requirement. Molecular print-based SPE is the most advanced application of MIPs [17].

Molecularly imprinted polymers (MIPs) are synthetic materials with high selectivity specific to the template molecule. Molecularly imprinted polymers are of interest to researchers because they have advantages such as increased affinity and selectivity to the target molecule, long-term retention of recognition capabilities, increased physical and chemical stability, as well as easy preparation. Molecularly imprinted polymers are used in many fields of chemistry, biology, and medicine as affinity material for sensors, in the production of artificial antibodies, the adsorbent in solid-phase extraction, and stationary phase in chromatography [18, 19].

This study aims to synthesize a molecularly imprinted polymer for the first time in which propineb, a dithiocarbamate fungicide, is used as a template and used as an SPE sorbent. Characterization studies of the synthesized polymer (MIP) and non-imprinted polymer (NIP) were performed to ensure optimal retention of the target analyte. In addition, the adsorption properties of the polymers were investigated, and the selective analysis of propineb from aqueous solutions was carried out as a result of their use as adsorbents in the SPE method.

Experimental section

Materials and apparatus

Propylenebis(dithiocarbamate) acid (propineb), methacrylic acid (MAA), ethylene glycol dimethacrylate (EGDMA), 2.2′-Azobis-isobutyronitrile (AIBN), polyvinyl alcohol (PVA), and solvents; dimethyl sulfoxide (DMSO), acetic acid, acetonitrile, chloroform, methanol were obtained from Sigma-Aldrich (USA). All solvents used were of analytic grade.

TGA/DSC analyses were determined using the Setaram Labsys Evo Gravimetric Analyzer 1600 model instrument. The surface morphology of the polymers was investigated using a scanning electron microscope (Zeiss Evo 15 Model). FTIR spectra were obtained with an FTIR Spectrometer (Bio-Rad-Win-IR Model). Adsorbent measurements were performed with the Optizen-POP model UV spectrophotometer.

Preparation of MIP and NIP

Imprinted polymer (MIP) was synthesized by suspension polymerization process using propineb as template molecule. At the synthesis stage, 0.5 mmol templates and 4 mmol MAA as functional monomer were dissolved in 40 mL DMSO in a glass vial and stirred at room temperature for 60 min. Then, 20 mmol of crosslinker EGDMA and 30 mg of initiator AIBN, and 200 mg of polyvinyl alcohol (PVA) dissolved in 25 mL of distilled water were added to the mixture and stirred for 15 min under a stream of nitrogen. The mixture was kept in an oil bath (70 °C) for 24 h (Fig. 1). The imprinted polymer was then extracted with a Soxhlet apparatus using 90:10 (v:v) methanol: acetic acid for 72 h to remove the template. After extraction, it was dried at 60 °C for 24 h [20]. The same procedure was used for preparing non-printed polymer (NIP) for MIP synthesis without the template molecule propineb.

MIP-SPE protocol

The applicability of the synthesized polymers was investigated by packing 50 mg of each polymer (MIP or NIP) into an empty 3.0-mL SPE cartridge. The cartridge was conditioned with MeOH (5 mL) and water (5 mL). 20 mL of propineb solution (25 mg/L) was passed through the SPE cartridge and washed with wash solution (3 mL) and then dried with airflow for 5 min. Then, the retained analytes were separated from the solid phase with 10 mL of eluent solution. All obtained fractions were collected and analyzed in a UV spectrophotometer at 232 nm. The same procedure was repeated using the commercial C_{18} cartridge, and the results were compared.

Binding experiments

Adsorption studies were carried out in 10 mL propineb solution (25 mg/L) with MIP and NIP. The pH of the propineb solution was adjusted between 4 and 10 using HCl or NaOH solutions. Then, 10 mg of polymer adsorbent was added to the propineb

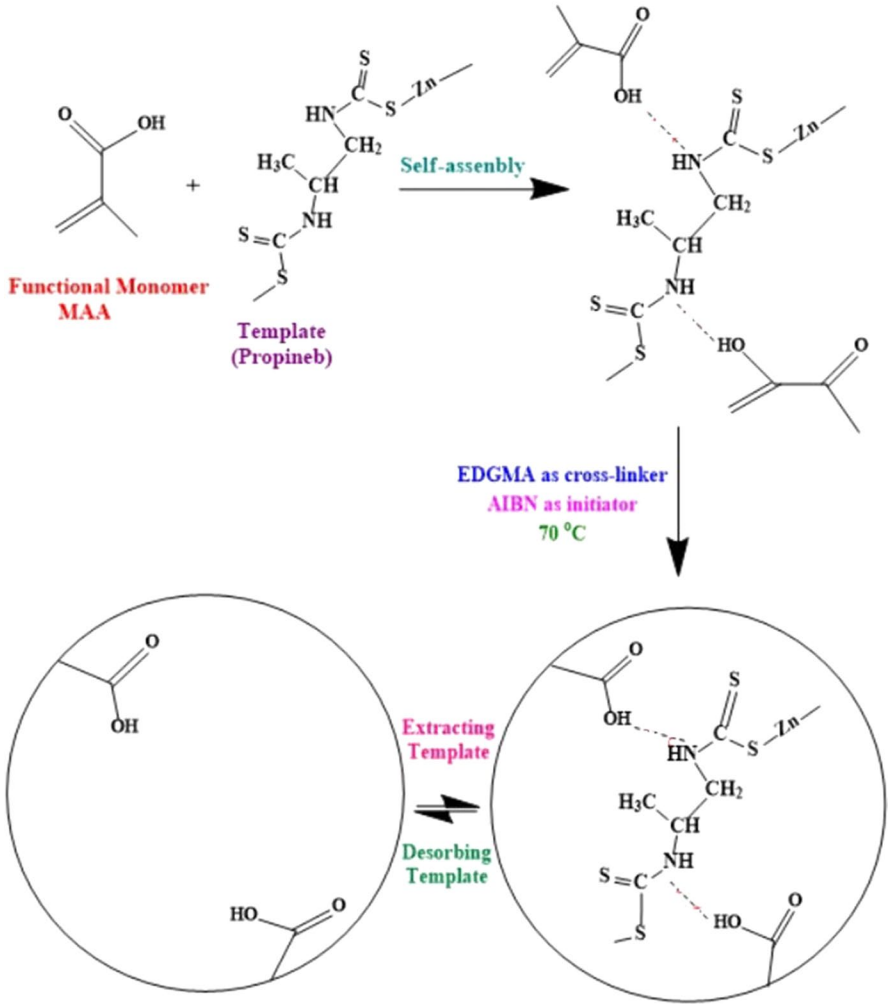

Fig. 1 Schematic representation of synthesis procedure of MIP

solution and shaken at 400 rpm and 25 °C. The amount of propineb adsorbed using the MIP and NIP was determined according to the following equations (Eqs. 2–3) [21]:

$$q = \left(C_o - C_e\right) \times V/m \tag{1}$$

$$\%R = \left(C_o - C_e\right)/C_o \times 100 \tag{2}$$

where q (mg/g) is the amount of propineb adsorbed on the adsorbent, C_o and C_e are the initial and equilibrium concentration (mg/L) of propineb in solution, respectively. R is removed yield (%). m (g) is the mass of adsorbent, and V (L) is the

volume of the propineb solution. At the end of the adsorption processes, the amount of propineb remaining in the solution was observed at 232 nm using a UV–Vis spectrophotometer.

The effect of pH on propineb adsorption was investigated in the range of 4–10 initial pH values. In studies conducted for MIP and NIP, the adsorption efficiency increased in the field of pH 4–6 and reached its maximum value at pH 6. Adsorption efficiency at pH 6 was determined as 89.32% for MIP and 48.2% for NIP. When pH > 6, a decrease in adsorption efficiency was observed; therefore, in further studies, the pH value six will be used.

Adsorption kinetics

The effect of contact time on propineb adsorption was investigated. The amount of adsorption obtained in MIP and NIP at an initial propineb concentration of 25 mg/L at pH 6, at room temperature, and at different adsorption times (between 5 and 240 min), is shown in Fig. 2. Propineb military remaining in solution at the end of the period was measured at 232 nm with a UV–Vis spectrophotometer. While the amount of adsorbed propineb increased in the first minutes of contact, equilibrium was reached in 30 min for MIP and NIP particles. A decrease in adsorption capacity over time was observed. This is because while the number of empty spaces that can be used on the adsorbent surface is high in the first stage, it becomes difficult for

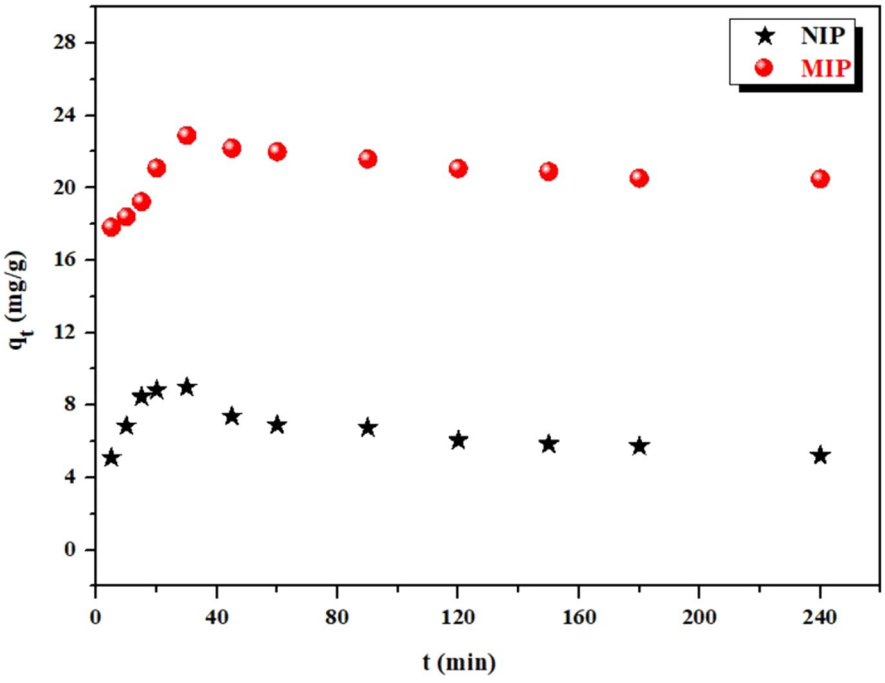

Fig. 2 Effect of contact time for propineb adsorption (pH = 6, T = 25 °C, C_0 = 25 mg/L, w = 10 mg)

propineb to adhere to the decreasing empty spaces due to the repulsive forces on the adsorbent surface as time progresses. The adsorption capacity of the MIP adsorbent, which has selective imprinting areas for propineb, was found to be higher than that of the unprinted polymer NIP.

The adsorbent's equilibrium time and the mechanism of action for removing propineb from wastewater are determined by examining the adsorption kinetics. The data obtained were analyzed using the pseudo-first-order model [22], pseudo-second-order model [23], and the intraparticle diffusion model [24]. The equations for the kinetic models are given below (Eqs. 3–5):

$$\text{Pseudo-first order}: \ln(q_e - q_t) = \ln q_e - k_1 \times t \tag{3}$$

$$\text{Pseudo-second order}: t/q_t = 1/k_2 \times q_e^2 + t/q_e \tag{4}$$

$$\text{Intra particle diffusion}: q_t = k_{id} \times t^{1/2} + I \tag{5}$$

where q_e and q_t are the quantity of propineb adsorbed in equilibrium, and at time t, respectively, k_1, k_2, and kid are the equilibrium rate constant of pseudo-first-order adsorption (1/min), pseudo-second-order adsorption (g/mg min), and intraparticle diffusion model (mg/g $\text{min}^{1/2}$), and it is the intercept.

Δq_e (%) is the normalized standard deviation. The best suited model can also specify the mean relative error (ARE) using [25, 26]. Equations were calculated for kinetic works as follows (6–7):

$$\Delta q_e\,(\%) = 100\sqrt{\frac{\sum\left[\left(q_{t,\text{exp}} - q_{t,\text{ calc}}\right)/q_{t,\text{exp}}\right]^2}{N-1}} \tag{6}$$

$$\text{ARE} = \frac{100}{N}\sum_{n=1}^{n}\left(\frac{q_{\text{exp}} - q_{\text{cal}}}{q_{\text{exp}}}\right) \tag{7}$$

where $q_{t,\text{exp}}$ and $q_{t,\text{calc}}$ (mg/g) are the experimental and the calculated adsorbed quantities at a given time t, respectively, q_{exp} and q_{cal} (mg/g) are the experimental and computed equilibrium adsorption capacity, respectively, N is the count of data points.

Results and discussion

Characterization of polymer

The constructive morphology of the imprinted polymer (MIP) and non-imprinted polymer (NIP) particles is shown in Fig. 3. From the figure, it can be seen that all particles have an irregular spherical shape. MIP surface contains larger particles that are more porous and packed with a rougher surface morphology (Fig. 3a). However,

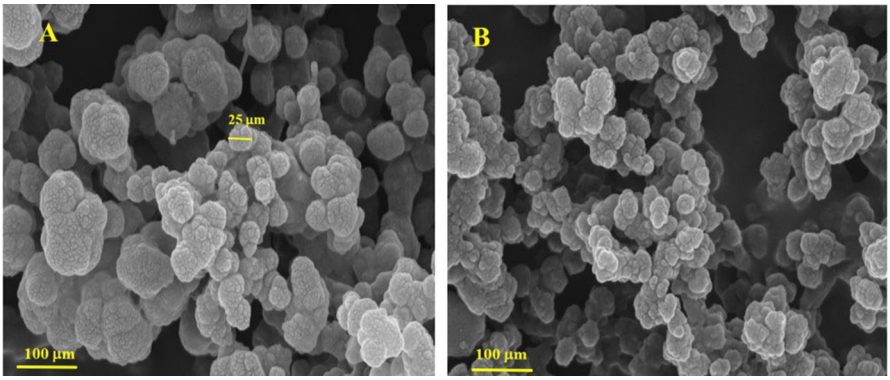

Fig. 3 SEM images of (magnification of 100,000) **a** MIP and **b** NIP

the NIP morphology contains densely packed particles with a smoother surface (Fig. 3b). This may be because no specific binding site is formed in the polymer particles without the propineb template. Porosity is an important factor because it enlarges the surface area of the sorbent by enabling the formation of new binding sites that play a role in the capture of analyte molecules and their selective removal from solutions [27, 28].

Thermogravimetric analysis results for MIP and NIP particles are shown in (Fig. 4). The samples were heated between 30 and 1000 °C at a heating rate of

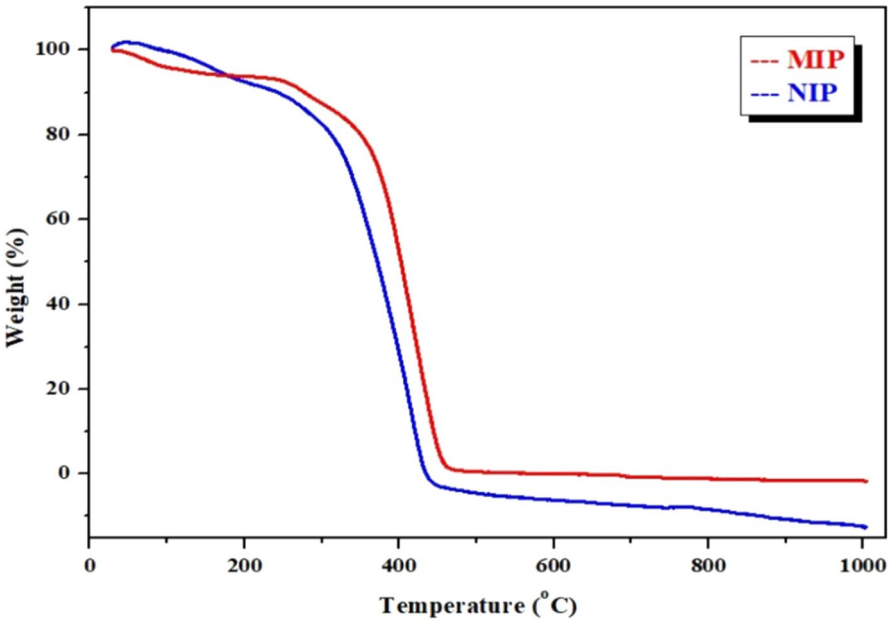

Fig. 4 Thermogravimetric curves of MIP and NIP

10 °C/min in an N_2 atmosphere in the measurement process. The figure shows a mass loss of approximately 6.7%, the main component of water, between 30 °C and 167 °C, similar for MIP and NIP. In addition, MIP decomposes rapidly from 246 °C to 484 °C, while NIP decomposes from 212 °C to 443 °C. Of the highly thermally stable MIP and NIP particles, the ultimate degradation temperature of MIP is relatively higher than the corresponding NIP, indicating that the MIP template is more stable at high temperatures [29].

FTIR characterization was performed to identify functional groups in NIP with MIP particles before and after the washing step (Fig. 5). Both MIP and NIP show similar spectra in a backbone structure. In interaction between template and monomer, a wide OH stretch band is observed at 3600–3200 cm^{-1} due to hydrogen-bonded amide (N–H) and a hydroxyl group (OH) [30, 31]. The peaks at ~ 2900 cm^{-1} are due to C-H stretching vibrations found in propineb, methacrylic acid, and EGDMA, and ~ 2995 cm^{-1} is the stretching vibrations of = C-H. Strong peaks at ~ 1720 cm^{-1} suggest the presence of –COOH of methacrylic acid. In addition, ~ 1635 cm^{-1}, ~ 1440 cm^{-1}, ~ 1300 cm^{-1} and ~ 1200 cm^{-1} peaks correspond to the presence of C=C stretching, $–CH_2$ stretching, CH_3 group and C–O stretching, respectively [32, 33]. The similarity of the spectra of the post-extraction NIP and MIP indicates that the polymerization procedure was carried out successfully [34].

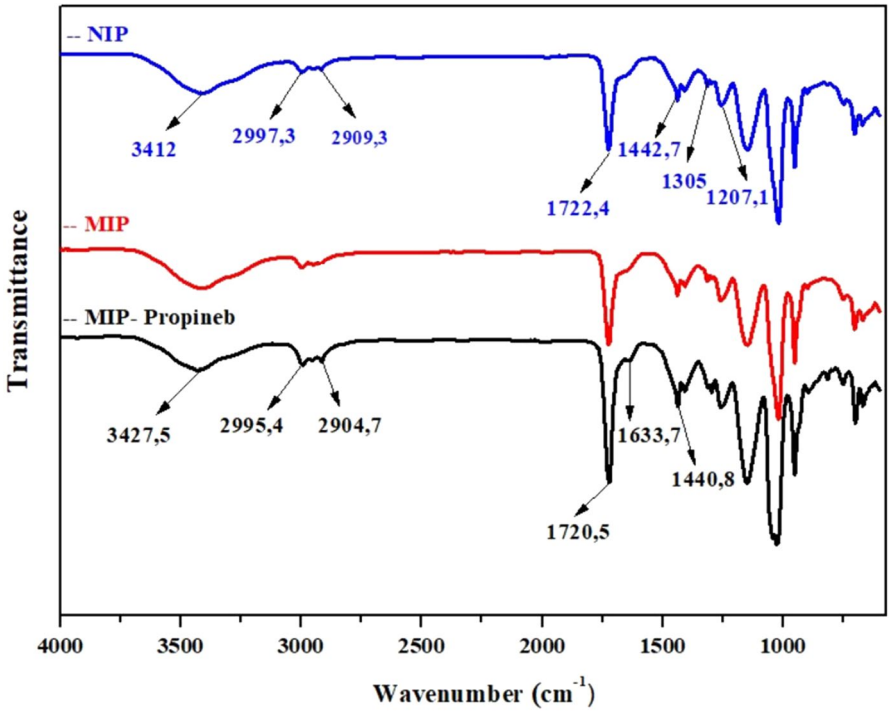

Fig. 5 FTIR spectra of loaded and unloaded MIPs and NIP

Optimization of MIP-SPE protocol

The effect of different experimental factors on the extraction efficiency was evaluated in order to increase the selectivity of MIP against NIP as well as the quantitative recovery of the target analyte. Amounts of MIP and NIP adsorbents ranging from 25 to 150 mg were tested as shown in Table 1. When the amount of adsorbent increased (from 25 to 50 mg), the amount of extracted propineb increased and the highest recovery (93%) and the best imprinting factor (2.12) were observed at the amount of 50 mg adsorbent. It was also noted that when the amount of adsorbent is more significant than 50 mg, there is a slight decrease in extracted propineb.

The purpose of using a wash solution is to wash any remaining interference from the sample matrix without separating the analytes. The choice of wash solvent to ensure a selective extraction of the analytes is an essential step in the extraction procedure as it eliminates unwanted matrix interactions. In general, the porogenic solvent is commonly used as a washing solvent [35]. Therefore, DMSO and water-DMSO mixtures are given in Table 1. As can be seen, the highest recovery (95.8%) and the best imprinting factor (1.94) were found in the water/DMSO (75/25: v/v). The optimal composition was thus: 3 mL water /DMSO (75/25: v/v).

The elution procedure was evaluated to achieve maximum propineb recovery using solutions of acetone, methanol, chloroform, acetonitrile, and methanol/acetic acid (95:05, 80:20, 75:25, v/v). The maximum extraction yield was observed in the methanol/acetic acid (95:05, v/v) mixture (96.4%). This may be because acetic acid added to methanol, which has a strong hydrogen bonding interaction with the analyte, disrupts the hydrogen bond between the analyte and MAA and facilitates analyte desorption by MeOH [36].

The volumes of elution solvents for MIP-SPE were studied at 1, 5, 10, 15, 20, 25, 30 mL, respectively. Experimental results showed that 10 mL is the optimum

Table 1 The effect of adsorbent amount and washing composition on imprinting factor and extraction recoveries in MIP-SPE method

Recovery (%)							
Adsorbent amounts (mg)	MIP	NIP	IF	Wash Solvents	MIP	NIP	IF
25	88.3	49.4	1.79	Water/ DMSO (100/0: v/v)	81.6	51.9	1.57
50	93	43.7	2.12	Water/ DMSO (80/20: v/v)	88.7	53.7	1.65
75	90.3	46.6	1.93	Water/ DMSO (75/25: v/v)	95.8	49.3	1.94
100	89.7	48.1	1.86	Water/ DMSO (50/50: v/v)	89	55	1.62
125	86	50.3	1.71	Water/ DMSO (25/75: v/v)	83.4	56.2	1.48
150	85.9	54	1.59	Water/ DMSO (20/80: v/v)	82.8	58	1.43

volume for maximum analyte elution. 10 mL of elution solvent provided recovery of the analyte from MIP with a high extraction efficiency of 97.3%.

Adsorption kinetic models

The parameters of the kinetic models are given in Table 2. When the results are examined, it is seen that the pseudo-second-order kinetic model is more suitable for both MIP and NIP for the adsorption process. Compared to other kinetic models, the correlation coefficient (R^2) is higher, and the difference between $q_{e,cal}$ values and experimental $q_{e,exp}$ is less. In the pseudo-first-order kinetic model, the difference between the $q_{e,calc}$ values and the experimental $q_{e,exp}$ values is significant, and the R^2 value is lower. Therefore, it can be said that adsorption does not occur by a pseudo-first-order process. It is seen that the standard deviation Δq_e (%) and ARE values calculated in the pseudo-second-order model are lower at all three concentration values. Therefore, this model was found to be more suitable for estimating experimental data on propineb adsorption.

The so-called second-order kinetic model is based on the assumption that the rate-limiting step may be chemisorption involving valence forces via sharing or electron exchange between propineb and adsorbents. According to this model, the adsorption rate of Propine on MIP and NIP adsorbents was primarily affected by the adsorption sites (functional groups) on the adsorbent [37]. The linearized graph in Fig. 6 shows that the charts for MIP and NIP are divided into two phases by two suitable curves. These results show that the intraparticle diffusion process is not the only rate control step during adsorption. For both adsorbent, in the first step, Propine in the solution was transported to the adsorbent surface (film diffusion), and

Table 2 Kinetic parameters of propineb adsorption on MIP and NIP

Models	Parameters	MIP	NIP
Pseudo-first order	$q_{e,\,cal}$ (mg/g)	14.12	4.85
	k_1 (1/min)	0.11	0.04
	R^2	0.9763	0.8981
	$q_{e,exp}$ (mg/g)	22.9	9.39
	Δq_e (%)	19.17	24.17
	ARE	7.67	9.67
Pseudo-second-order	$q_{e,\,cal}$ (mg/g)	20.82	5.78
	k_2 (g/mg.min)	0.09	0.01
	R^2	0.9949	0.9829
	$q_{e,exp}$ (mg/g)	22.9	9.39
	Δq_e (%)	4.54	19.22
	ARE	1.82	7.69
Weber-Morris intra-particle diffusion	k (mg/g.min$^{1/2}$)	1.75	0.95
	I (mg/g)	5.32	1.52
	R^2	0.9716	0.8962

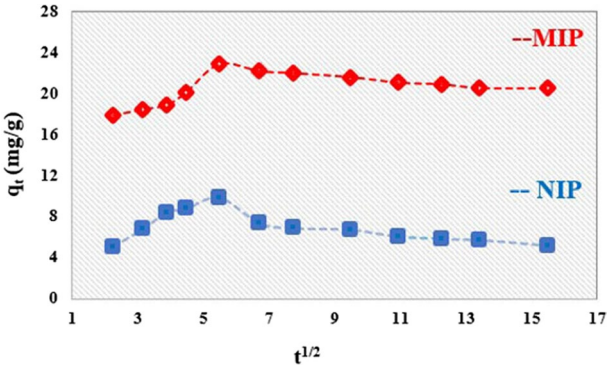

Fig. 6 Intraparticle diffusion kinetic model plots of MIP and NIP for propineb adsorption

in the second step, propineb molecules were transferred from the outer surface and adsorbed into the pores of the adsorbent (intraparticle diffusion) [38, 39].

Regeneration of MIP

Adsorption performance was evaluated after repeated cycles to assess the regeneration and reuse capacity of MIP. It was measured spectrophotometrically after 30 min in propineb solution, and the MIP particles were washed for 5 min with 10 mL of methanol/acetic acid solution (9:1, v/v). This procedure was repeated for five cycles; the results were compared to unregenerated MIP particles (Fig. 7). In this figure, the percentage of propineb adsorbed within 30 min due to the presence of regenerated and non-regenerated MIP, respectively, is indicated. The results show that MIP can be efficiently reused thanks to the regeneration process as it retains its adsorption capacity. Still, if regeneration does not occur, the adsorbing capacity of the fungicide will be greatly reduced after only four cycles. The mild decrease in MIP adsorption performances is due to a gradual loss of particles during the washing steps.

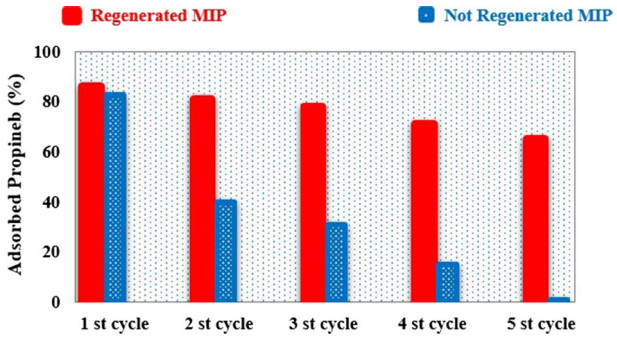

Fig. 7 Adsorption cycles by a regenerated MIP and not regenerated MIP

Statistical comparing of SPE procedures

The *t*-test, a statistical hypothesis test, was applied to determine the possibility that the MIP-SPE method would differ considerably from the NIP-SPE and commercial C_{18}-SPE methods. 25 mg/L solutions of propineb were used for all three methods under optimum conditions, and the obtained recovery values and *p* values are shown in Table 3. Recovery values are 98.34% for MIP-SPE, 83.14% for C_{18}-SPE, and 50.3% for NIP-SPE. For the independent *t*-test, the *p*-value is 0.0037 for comparing MIP-SPE with commercial C_{18}-SPE, while the *p*-value is 0.0007 for the comparison of MIP-SPE and NIP-SPE. The null hypothesis was rejected as *p* values were less than $\alpha = 0.05$ in both comparison cases [36]. Accordingly, MIP-SPE data values differ considerably from NIP-SPE and C_{18}-SPE methods.

Conclusion

In this study, by suspension polymerization method, using methacrylic acid (MAA) as a functional monomer and ethylene glycol dimethacrylate (EGDMA) as a crosslinker, a MIP for the template molecule propineb was synthesized for the first time. The mole ratio of template molecule/monomer/crosslinker was determined as 0.5:4:20. In addition, NIP was synthesized as a reference. The MIP and NIP prepared by the suspension polymerization method were characterized by SEM, TGA, and FTIR, for the morphology, thermal stability, and bonding, respectively. As a result of kinetic studies, it was determined that propineb adsorption was more compatible with the pseudo-second-order kinetic model. With an easy and fast procedure, the selectivity of the adsorption process and the reusability of the synthesized MIP sorbent were demonstrated after several adsorption/regeneration cycles.

The high extraction efficiency of 98.7% was obtained in the SPE method, in which MIP is also used as a solid phase and provides less time and solvent consumption. In addition, it was determined that MIP-SPE data values were quite differ from C_{18}-SPE and NIP-SPE methods under optimized extraction conditions. This study is also essential in the literature as it is rare adsorption and solid-phase extraction study using propineb.

As a result, it is essential to develop new selective materials with molecular recognition mechanisms to isolate pesticides that threaten environmental health from complex environmental matrices. Solid-phase extraction processes using molecularly imprinted polymers with selectivity and high affinity against a certain

Table 3 Recovery study and comparing of *p*-value *t*-test and statistical method (*t*-test)

Analyte	Recoveries (%)		*p*-value	Recoveries (%)		*p*-value
	MIP-SPE	C_{18}-SPE		MIP-SPE	NIP-SPE	
Propineb	98.34	83.14	0.0037	98.34	50.3	0.0007

analyte are highly beneficial for the selective and easy removal of environmental pollutants such as pesticides.

Acknowledgements This work was supported by the Van Yuzuncu Yil University Scientific Research Projects Support Unit (Project Number: 8444).

Declarations

Conflict of interest The authors declare that they have no known competing financial interests or personal relationships that could have influenced the work reported in this paper.

References

1. Abbaci A, Azzouz N, Bouznit Y (2014) A new copper doped montmorillonite modified carbon paste electrode for propineb detection. Appl Clay Sci 90:130–134
2. Kazos EA, Stalikas CD, Nanos CG, Konidari CN (2007) Determination of dithiocarbamate fungicide propineb and its main metabolite propylenethioureain airborne samples. Chemosphere 68:2104–2110
3. Commission E (2002) Pesticide. Food Safety Residue, Brussels
4. FAO/WHO (1993) Pesticides residues in food. Evaluations. Part II-toxicology. Joint FAO/WHO Meeting on Pesticides Residues, Geneva, Switzerland, 20–29 September 1993.
5. Richardson ML, Gangolli S (1997) The dictionary of substances and their effects. The Royal Society of Chemistry, Cambridge, UK
6. Sharma D, Nagpal A, Pakade YB, Katnoria JK (2010) Analytical methods for estimation of organophosphorus pesticide residues in fruits and vegetables: a review. Talanta 82:1077–1089
7. Guan WN, Wang YJ, Xu F, Guan YF (2008) Poly (phthalazine ether sulfone ketone) as novel stationary phase for stir bar sorptive extraction of organochlorine compounds and organophosphorus pesticides. J Chromatogr A 1177:28–35
8. Rodrigues FM, Mesquita PRR, Oliveira LS, Oliveira FS, Filho AM et al (2011) Development of a headspace solid-phase microextraction/gas chromatography–mass spectrometry method for determination of organophosphorus pesticide residues in cow milk. Microchem J 98:56–61
9. Topuz S, Ozhan G, Alpertunga B (2005) Simultaneous determination of various pesticides in fruit juices by HPLC-DAD. Food Control 16:87–92
10. Liu M, Hashi Y, Song Y, Lin JM (2005) Simultaneous determination of carbamate and organophosphorus pesticides in fruits and vegetables by liquid chromatography mass spectrometry. J Chromatogr A 1097:183–187
11. Du JJ, Gao RX, Yu H, Li XJ, Mu H (2015) Selective extraction of dimethoate from cucumber samples by use of molecularly imprinted microspheres. J Pharm Anal 5:200–206
12. Li JW, Wang YL, Yan S, Li XJ, Pan SY (2016) Molecularly imprinted calixarene fiber for solid-phase microextraction of four organophosphorous pesticides in fruits. Food Chem 192:260–267
13. Naeeni MH, Yamini Y, Rezaee M (2011) Combination of supercritical fluid extraction with dispersive liquid–liquid microextraction for extraction of organophosphorus pesticides from soil and marine sediment samples. J Supercrit Fluid 57:219–226
14. Bidari A, Ganjali MR, Norouzi P, Hosseini MRM, Assadi Y (2011) Sample preparation method for the analysis of some organophosphorus pesticides residues in tomato by ultrasound-assisted solvent extraction followed by dispersive liquid–liquid microextraction. Food Chem 126:1840–1844
15. Rodriguez-Mozaz S, Lopez de Alda MJ, Barcelo D (2007) Advantages and limitations of on-line solid phase extraction coupled to liquid chromatography-mass spectrometry technologies versus biosensors for monitoring of emerging contaminants in water. J Chromatogr A 1152:97–115
16. Zhu XL, Yang J, Su QD, Cai JB, Gao Y (2005) Selective solid-phase extraction using molecularly imprinted polymer for the analysis of polar organophosphorus pesticides in water and soil samples. J Chromatogr A 1092:161–169
17. Sergeyeva TA, Matuschewski H, Piletsky SA, Bendig J, Schedler U, Ulbricht M (2001) Molecularly imprinted polymer membranes for substance-selective solid-phase extraction from water by surface photo-grafting polymerization. J Chromatogr A 907:89–99
18. He C, Long Y, Pan J (2007) Application of molecularly imprinted polymers to solid-phase extraction of analytes from real samples. J Biochem and Biophys Methods 70:133–150

19. Vasapollo G, Sole R (2011) Molecularly imprinted polymers: present and future prospective. Int J Mol Sci 12:5908–5945
20. Soysal M, Karagözler AE (2018) Voltammetric determination of thiuram by carbon paste electrodes modified with molecular imprinted polymers. Eur J Sci Technol 14:323–333
21. Ge H, Wang C, Liu S et al (2016) Synthesis of citric acid functionalized magnetic graphene oxide coated corn straw for methylene blue adsorption. Bioresour Technol 221:419–429
22. Lagergren S (1898) About the theory of so-called adsorption of soluble substances. Kungl Svens Vetensk Akad Handl 24:1–39
23. Ho YS, McKay G (1999) Pseudo-second order model for sorption processes. Process Biochem 34:451–465
24. Weber WJ, Morris JC (1963) Kinetics of adsorption on carbon from solution. J Sanit Eng Div 89:31–60
25. Cazetta A, Vargas A, Nogami E, Kunita M, Guilherme M, Martins A, Silva T, Moraes J, Almeida V (2011) NaOH-activated carbon of high surface area produced from coconut shell: kinetics and equilibrium studies from the methylene blue adsorption. Chem Eng J 174:117–125
26. Guo F, Li X, Jiang X, Zhao X, Guo C, Rao Z (2018) Characteristics and toxic dye adsorption of magnetic activated carbon prepared from biomass waste by modified one-step synthesis. Colloids Surf A 555: 43–54
27. Shahera Khairi NA, Yusof NA, Abdullah AH, Mohammad F (2015) Removal of toxic mercury from petroleum oil by newly synthesized molecularly-imprinted polymer. Int J Mol Sci 16:10562–10577
28. Chen Y, Zheng X, Qian H, Mao Z, Ding D, Jiang X (2010) Hollow core-porous Shell structure poly (acrylic acid) nanogels with a superhigh capacity of drug loading. ACS Appl Mater Interfaces 2:3532–3538
29. Yusof NA, Rahman SKA, Hussein MA, Ibrahim NA (2013) Preparation and characterization of molecularly imprinted polymer as SPE sorbent for melamine isolation. Polymer 5:1215–1228
30. Mei XQ, He XP, Wang JT (2016) Molecularly imprinted polymer as efficient sorbent of solid-phase extraction for determination of gonyautoxin 1,4 in seawater followed by high-performance liquid chromatography-fluorescence detection. Anal Bioanal Chem 408:5737–5743
31. Brune BJ, Koehler JA, Smith PJ, Payne GF (1999) Correlation between adsorption and small molecule hydrogen bonding. Langmuir 15:3989–3992
32. Shafqat SR, Bhawani SA, Bakhtiar S, Ibrahim MNM (2020) Synthesis of molecularly imprinted polymer for removal of Congo red. BMC Chemistry 14:1–15
33. Bashir S, Teo YY, Ramesh S, Ramesh K (2016) Synthesis, characterization, properties of N-succinyl chitosan-g-poly (methacrylic acid) hydrogels and in vitro release of theophylline. Polymer 92:36–49
34. Xu Z, Fang G, Wang S (2010) Molecularly imprinted solid phase extraction coupled to high-performance liquid chromatography for determination of trace dichlorvos residues in vegetables. Food Chem 119:845–850
35. Binsalom A, Chianella I, Campbell K, Zourob M (2016) Development of solid-phase extraction using molecularly imprinted polymer for the analysis of organophosphorus pesticides-(chlorpyrifos) in aqueous solution. J Chromatogr Sep Sci 7:1–6
36. Sanagi MM, Salleh S, Ibrahim WAW, Naim AA, Hermawan D, Miskam M, Hussain I, Aboul-Enein HY (2013) Molecularly imprinted polymer solid-phase ex- traction for the analysis of organophosphorus pesticides in fruit samples. J Food Comp Anal 32:155–161
37. Zhou L, Huang Z, Luo T, Jia Y, Liu Z, Adesina AA (2015) Biosorption of uranium(VI) from aqueous solution using phosphate-modified pine wood sawdust. J Radioanal Nucl Chem 303:1917–1925
38. Wong K, Eu N, Ibrahim S, Kim H, Yoon Y, Jang (2020). Recyclable magnetite-loaded palm shell-waste based activated carbon for the 3 effective removal of methylene blue from aqueous solution. J Clean Prod
39. Ma X, Liu C, Anderson DP, Chang PR (2016) Porous cellulose spheres: preparation, modification and adsorption properties. Chemosphere 165:399–408